

2012

Structural Characterization of a Conserved, Calcium-Dependent Periplasmic Protease from *Legionella pneumophila*


Debashree Chatterjee
Cornell University

Chelsea D. Boyd
Dartmouth College

George A. O'Toole
Dartmouth College

Holger Sondermann
Dartmouth College

Follow this and additional works at: <https://digitalcommons.dartmouth.edu/facoa>

 Part of the [Bacteriology Commons](#), and the [Medical Microbiology Commons](#)

Recommended Citation

Chatterjee, Debashree; Boyd, Chelsea D.; O'Toole, George A.; and Sondermann, Holger, "Structural Characterization of a Conserved, Calcium-Dependent Periplasmic Protease from *Legionella pneumophila*" (2012). *Open Dartmouth: Faculty Open Access Articles*. 1051.
<https://digitalcommons.dartmouth.edu/facoa/1051>

This Article is brought to you for free and open access by Dartmouth Digital Commons. It has been accepted for inclusion in Open Dartmouth: Faculty Open Access Articles by an authorized administrator of Dartmouth Digital Commons. For more information, please contact dartmouthdigitalcommons@groups.dartmouth.edu.

Structural Characterization of a Conserved, Calcium-Dependent Periplasmic Protease from *Legionella pneumophila*

Debashree Chatterjee,^a Chelsea D. Boyd,^b George A. O'Toole,^b and Holger Sondermann^a

Department of Molecular Medicine, College of Veterinary Medicine, Cornell University, Ithaca, New York, USA,^a and Department of Microbiology and Immunology, Geisel School of Medicine at Dartmouth, Hanover, New Hampshire, USA^b

The bacterial dinucleotide second messenger c-di-GMP has emerged as a central molecule in regulating bacterial behavior, including motility and biofilm formation. Proteins for the synthesis and degradation of c-di-GMP and effectors for its signal transmission are widely used in the bacterial domain. Previous work established the GGDEF-EAL domain-containing receptor LapD as a central switch in *Pseudomonas fluorescens* cell adhesion. LapD senses c-di-GMP inside the cytosol and relays this signal to the outside by the differential recruitment of the periplasmic protease LapG. Here we identify the core components of an orthologous system in *Legionella pneumophila*. Despite only moderate sequence conservation at the protein level, key features concerning the regulation of LapG are retained. The output domain of the LapD-like receptor from *L. pneumophila*, CdgS9, binds the LapG ortholog involving a strictly conserved surface tryptophan residue. While the endogenous substrate for *L. pneumophila* LapG is unknown, the enzyme processed the corresponding *P. fluorescens* substrate, indicating a common catalytic mechanism and substrate recognition. Crystal structures of *L. pneumophila* LapG provide the first atomic models of bacterial proteases of the DUF920 family and reveal a conserved calcium-binding site important for LapG function.

Bacteria sense and respond to their environment by a multitude of physiological programs, allowing them to adapt to changing and often hostile conditions. Biofilm formation is one such mechanism that is used widely by many pathogenic and environmental bacteria (16). c-di-GMP, a molecule unique to bacteria, has emerged as an important intracellular second messenger that regulates the formation of biofilms at multiple levels (17). The majority of the bacterial genomes sequenced to date encode enzymes for the production and turnover of c-di-GMP, diguanylate cyclases with GGDEF domains, and phosphodiesterases with EAL or HD-GYP domains, respectively (12). Receptors for c-di-GMP are a less-well-defined group that includes receiver domains in transcription factors, PilZ domain-containing proteins, riboswitches, and proteins with catalytically inactive GGDEF or EAL domains constituting a distinct class (36). These proteins exploit their degenerate active sites or regulatory c-di-GMP-binding sites to sense the cellular concentration of the dinucleotide and to solicit a specific response.

One such receptor, the transmembrane protein LapD from *Pseudomonas fluorescens*, contains both catalytically inactive GGDEF and EAL domains, with the latter serving as the exclusive c-di-GMP binding module (31). Previous work established LapD as a prototypical receptor for mediating inside-out signaling from the cytosol to the periplasm. LapD responds to a rise in c-di-GMP levels triggered by a nutritional signal, namely, the availability of P_i, by undergoing a conformational change from a nucleotide-free, autoinhibited state to a c-di-GMP-activated state (19, 28–30) (Fig. 1A). Only the activated state is capable of sequestering a periplasmic protease, LapG, to LapD's output domain which, in turn, stabilizes LapG's substrate, LapA (30). LapA is a large adhesin protein that is embedded in the outer membrane by an unknown mechanism (18). Proteolytic processing by LapG releases LapA from the membrane, leading to biofilm dispersion when P_i is limiting (30). In conjunction with revealing the signaling and output system for biofilm formation in *P. fluorescens*, we determined the crystal structures of the functional domains of LapD spanning almost the entire receptor (29). These studies revealed the main

regulatory features controlling LapD function. Based on a bioinformatic analysis, it also allowed us to predict orthologous signaling systems in many other bacteria, which may hinge on a LapD-like c-di-GMP receptor and a LapG-like protease. Two of these have been characterized independently in *Pseudomonas putida* and *Shewanella oneidensis* (14, 37).

Another orthologous system that we predicted, based on bioinformatics, is that of *Legionella pneumophila*, the causative agent of Legionnaires' disease (29). Unlike *Pseudomonas*, *L. pneumophila* is a facultative intracellular bacterium that is also able to grow in biofilms. Its genome encodes 21 predicted proteins with GGDEF and/or EAL domains and a single PilZ protein, and a subset of these have been shown to impact intracellular growth, motility, or biofilm formation (5, 25, 34). However, the underlying signaling mechanisms and networks and their regulation are largely unknown for the majority of these proteins.

In this study, we focused on the periplasmic protease LapG of *L. pneumophila*. LapG belongs to the domain of unknown function 920 (DUF920) (or COG3672) family, and hence, little is known regarding its molecular mechanism. Sequence and fold recognition methods classified these proteins as bacterial transglutaminase-like cysteine proteases (BTLCPs) and predicted a cysteine-histidine-aspartate (C-H-D) catalytic triad and core structural motifs at the active site (13). Recently, O'Toole and colleagues corroborated the notion that LapG functions as a cysteine protease (30). In an effort to further our mechanistic understanding of LapG and related proteases, we determined crystal

Received 16 April 2012 Accepted 8 June 2012

Published ahead of print 15 June 2012

Address correspondence to Holger Sondermann, hs293@cornell.edu.

Supplemental material for this article may be found at <http://jb.asm.org/>.

Copyright © 2012, American Society for Microbiology. All Rights Reserved.

doi:10.1128/JB.00640-12

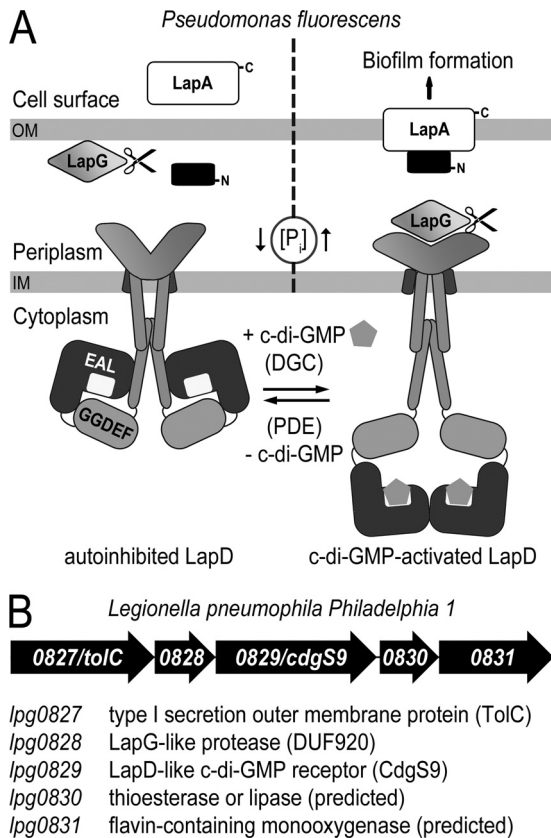


FIG 1 The LapADG signaling system. (A) Model of LapD-mediated regulation of biofilm formation in *P. fluorescens*. The c-di-GMP receptor LapD localizes to the inner membrane (IM), where it senses cytoplasmic c-di-GMP levels. It controls the stability of the large adhesin LapA in the outer membrane (OM) by sequestration of the periplasmic protease LapG. The underlying signaling pathway is controlled by the availability of P_i. (B) Genetic map of the LapD ortholog-containing operon in *L. pneumophila*.

structures of the LapG ortholog from *L. pneumophila*. In a parallel study, the O'Toole group noted a dependence of *P. fluorescens* LapG activity on calcium ions (4), and the structures allowed us to identify a strictly conserved calcium-binding site in LapG and BTLCs. In addition, we demonstrate that the *L. pneumophila* LapD-LapG system utilizes an output mechanism similar to that which we previously described in *P. fluorescens* (29, 30).

MATERIALS AND METHODS

Protein expression and purification. DNA fragments encoding *L. pneumophila* LapG lacking the signal peptide (*lpg0828*; residues 52 to 244) and the periplasmic output domain of the LapD ortholog CdgS9 (*lpg0829*; residues 22 to 152) were amplified from genomic DNA by standard PCR and cloned into a bacterial expression vector based on pET28a (Novagen) that adds an N-terminal, cleavable His₆-SUMO tag (see Table S1 in the supplemental material).

Native and selenomethionine-derivatized proteins were overexpressed in *Escherichia coli* BL21 T7 Express or T7 Express Crystal cells (New England BioLabs), respectively. For the expression of native proteins, cultures were grown at 37°C in terrific broth medium supplemented with 50 μg/ml kanamycin. At an optical density at 600 nm (OD₆₀₀) of ~1, the temperature was reduced to 18°C and protein expression was induced by adding 1 mM IPTG. Selenomethionine-derivatized proteins were expressed in cells grown at 37°C in M9 minimal medium supplemented with 50 μg/ml kanamycin, vitamins (1 μg/ml thiamine and 1 μg/ml biotin), a

carbon source (0.4% glucose), trace elements, and amino acids (each of the 20 amino acids at 40 μg/ml, with selenomethionine substituting for methionine). Protein expression was induced at an OD₆₀₀ of 0.4 to 0.5. In both cases, protein expression proceeded for 16 h at 18°C, after which cells were harvested by centrifugation, resuspended in Ni-nitrilotriacetic acid (NTA) buffer A (25 mM Tris-HCl [pH 8.5], 500 mM NaCl, 20 mM imidazole), and flash frozen in liquid nitrogen. Cell suspensions were thawed and lysed by sonication. Cell debris was removed by centrifugation, and the clear lysates were incubated with Ni-NTA resin (Qiagen) that was pre-equilibrated with Ni-NTA buffer A. The resin was washed with 20 column volumes of buffer A, followed by protein elution with 5 column volumes of Ni-NTA buffer B (25 mM Tris-HCl [pH 8.5], 500 mM NaCl, 300 mM imidazole). The eluted proteins were buffer exchanged into a low-salt buffer (25 mM Tris-HCl [pH 8.5], 150 mM NaCl) on a fast desalting column (GE Healthcare). Proteins were subjected to size exclusion chromatography on a Superdex 200 column (GE Healthcare) pre-equilibrated with gel filtration buffer (25 mM Tris-HCl [pH 8.5], 150 mM NaCl). Where indicated, the His₆-SUMO moiety was cleaved off by using the yeast protease Ulp-1 following desalting. Ulp-1, uncleaved protein, and the cleaved fusion tags were removed by Ni-NTA affinity chromatography prior to the final gel filtration. Purified proteins were concentrated on Amicon filters with an appropriate size cutoff to concentrations of >25 mg/ml, flash frozen in liquid nitrogen, and stored at -80°C.

The expression and purification of the corresponding proteins from *P. fluorescens* were described previously (29). The construction, expression, and purification of *P. fluorescens* LapA^{Nterm} were described elsewhere (30). Site-directed mutagenesis was carried out by using the QuikChange kit (Agilent Technologies) and following the manufacturer's instructions, followed by validation through DNA sequencing.

Crystallization, data collection, and structure solution. Crystals were obtained by hanging-drop vapor diffusion mixing equal volumes of protein (10 to 30 mg/ml) and reservoir solution, followed by incubation at 4°C. For the native, apo-state crystal form, the reservoir solution contained 0.14 M ammonium tartrate dibasic and 20% polyethylene glycol 3350. The selenomethionine-derivatized protein crystallized in the same condition supplemented with 0.1 M Bis-tris (pH 7.0). Crystals for calcium-bound and EGTA-treated LapG were obtained in the same condition as the apoprotein, supplemented with 2 mM CaCl₂ and EGTA, respectively. For cryoprotection, crystals were soaked in reservoir solution supplemented with 25% xylitol. Cryopreserved crystals were flash frozen and stored in liquid nitrogen. For optimal diffraction, crystals of LapG-Ca²⁺ were grown at 20°C and transferred to 4°C for 1 h prior to cryoprotection and freezing. Data on frozen crystals were collected at 100 K using synchrotron radiation at the Cornell High Energy Synchrotron Source (CHESS; Cornell University, Ithaca, NY).

Data reduction was carried out with the software package HKL2000 (33). Experimental phases for the initial structure determination were obtained from single-wavelength anomalous diffraction (SAD) experiments with crystals grown from selenomethionine-derivatized proteins by using the software package PHENIX (2). Refinement in PHENIX and COOT (11) yielded the final models. Data collection and refinement statistics are summarized in Table S2 in the supplemental material. Illustrations were made in Pymol (Schrödinger). Alignments were generated using ClustalW2 (24) and formatted with ESPript (15). Sequence logos were generated using WebLogo (8, 35).

Protein pull-down assay. His₆-SUMO-tagged *L. pneumophila* LapG or His₆-tagged *P. fluorescens* LapG was incubated with Ni-NTA resin (Qiagen) for 1 h at 4°C in binding buffer (25 mM Tris-HCl [pH 8.5], 75 mM NaCl, 25 mM KCl, 40 mM imidazole). Following the removal of unbound protein by three washing steps with 5 column volumes of binding buffer each, LapG-bound resin (corresponding to ~50 μg of protein) was incubated with an excess of the untagged output domain (250 μg or 20 μM) of either *L. pneumophila* or *P. fluorescens* LapD for 30 min at 4°C. After the resin was washed three times with 5 column volumes of binding buffer, proteins were eluted from the resin with elution buffer (25 mM Tris-HCl

[pH 8.5], 500 mM NaCl, 300 mM imidazole). Eluates were analyzed using standard denaturing SDS-PAGE and Coomassie staining. All incubations were carried out under gentle agitation in spin columns.

LapA cleavage assay. Purified *P. fluorescens* LapG variants (wild type or D¹³⁶A; 0.4 μM) and *L. pneumophila* LapG variants (wild type, D¹³⁶A, E¹³⁸A, or D¹³⁹A; 40 to 150 μM) were incubated at the indicated concentrations with purified LapA^{Nterm} (2 μM) in reaction buffer (25 mM Tris-HCl [pH 8.5], 150 mM NaCl, 20 mM MgCl₂) overnight at room temperature in the presence or absence of 10 mM EGTA. The reaction products were separated by SDS-PAGE and analyzed by Western blotting using a monoclonal antibody raised against pentahistidine (Qiagen) which was detected by a horseradish peroxidase-coupled anti-mouse antibody. Blots were developed by using enhanced chemiluminescence (GE Healthcare) and exposed to film.

SEC-MALS. Size exclusion chromatography-coupled multiangle light scattering (SEC-MALS) measurements were carried out by injecting purified proteins (100 μM) onto a WTC-030S5 gel filtration column (Wyatt Technology) preequilibrated with gel filtration buffer (25 mM Tris-HCl [pH 8.5], 150 mM NaCl). The SEC system was coupled to an 18-angle, static light scattering detector and a refractive index detector (DAWN HELEOS-II and Optilab T-rEX, respectively; Wyatt Technology). Data were collected at 25°C every second at a flow rate of 1 ml/min and analyzed with the software ASTRA, yielding the molecular mass and mass distribution (polydispersity) of the samples. For data quality control and normalization of the light scattering detectors, monomeric bovine serum albumin (Sigma) was used.

ITC. Isothermal titration calorimetry (ITC) was used to determine the apparent dissociation constants (K_d) and stoichiometry of interactions using a VP calorimeter (Microcal). Calorimetric titrations of calcium (2 mM in the syringe; 10-μl injections) and wild-type or mutant *L. pneumophila* LapG (200 μM in the cuvette) were carried out at 20°C in gel filtration buffer (25 mM Tris-HCl [pH 8.5], 150 mM NaCl) with a delay of 300 s between injections. The data obtained were analyzed by integrating heat effects normalized to the amount of injected protein and curve fitting based on a single-site binding model by using the Origin software package (Microcal).

Protein structure accession numbers. Coordinates and structure factors have been deposited in the Protein Data Bank (PDB) and assigned accession numbers 4FGQ, 4FGP, and 4FGO.

RESULTS

The Lap operon in *L. pneumophila*. We previously predicted the existence of proteins with sequence similarity to *P. fluorescens* LapD and LapG in several bacterial species, including *L. pneumophila* (29). *In silico* genomic analysis indicates that both genes map to an operon containing at least five genes (Fig. 1B). It encodes a predicted type I secretion outer membrane protein (*lpg0827*/TolC), a LapG-like protease (*lpg0828*), a LapD ortholog with a degenerate GGDEF-EAL domain module (*lpg0829*/CdgS9), and two putative proteins (*lpg0830*, predicted thioesterase/lipase activity; *lpg0831*, predicted flavin-containing monooxygenase). While the functional relevance of the latter two gene products within this cluster remains to be established, a type I secretion system is required in *P. fluorescens* for the translocation of the LapG substrate to the outer membrane (18), and *L. pneumophila* TolC may fulfill a similar function. Considering the limited mechanistic characterization of DUF920-containing proteins and the importance of LapG as a part of a c-di-GMP-dependent signaling system (29, 30), we set out to determine the molecular mechanism and structure of a LapG ortholog.

Conservation of the LapD-LapG interaction in *L. pneumophila*. To establish that the LapG and LapD orthologs indeed form a complex as part of a regulatory system, we cloned, expressed, and

purified the periplasmic output domain of *L. pneumophila* CdgS9 (the LapD ortholog) and LapG. Both proteins were expressed most stably with cleavable, N-terminal hexahistidine-SUMO (His₆-SUMO) tags. For comparison, we used the respective protein constructs from *P. fluorescens*, with the exception that LapG contained a C-terminal His₆ tag instead of the His₆-SUMO tag (29). We previously demonstrated that the interaction between *P. fluorescens* LapG and LapD relies on a strictly conserved, surface-exposed tryptophan residue that is present at the tip of a beta-hairpin motif in LapD's output domain (29) (Fig. 2A). Mutation of this residue (e.g., to alanine or glutamate) abolished LapG binding and signaling through LapD, serving as an invaluable specificity control.

His₆-tagged (or His₆-SUMO-tagged) LapG orthologs were bound to Ni-NTA Sepharose, washed, and incubated with the purified, untagged output domain of LapD or CdgS9, respectively. Proteins were eluted and analyzed by SDS-PAGE. Despite overall low sequence conservation of LapD orthologs (~23% across the entire receptor), *P. fluorescens* LapG adsorbed not only the cognate LapD output domain but also equally efficiently the corresponding domain of the *L. pneumophila* ortholog (Fig. 2B). A similar complex formation by *L. pneumophila* LapG and the corresponding LapD output domain was observed. Binding of *L. pneumophila* LapG to the output domain of *P. fluorescens* LapD was detectable but weaker. All interactions were sensitive to a non-conservative (W-to-E) mutation at the critical tryptophan residue at the center of the output domain beta-hairpin motif, indicating that the mode of binding is specific and conserved across distantly related bacterial species (Fig. 2B).

The crystal structure of *L. pneumophila* LapG. The LapG ortholog from *L. pneumophila* (residues 52 to 244; lacks the signal peptide) was expressed in *E. coli* as a soluble protein and purified by standard liquid chromatography. Upon crystallization (space group P2₁2₁2; two molecules per asymmetric unit), the high-resolution structure was determined by SAD phasing with selenomethionine-substituted protein crystals (Fig. 3A; see Table S2 in the supplemental material).

The structure reveals a bilobal fold of LapG (Fig. 3A). The N-terminal lobe is formed by five α-helices folding into a globular structure. In contrast, the C-terminal lobe consists of a five-stranded anti-parallel β-sheet. The three central strands are longer than the two flanking strands. The extreme C terminus folds into a helix that is connected to the bulk of the protein by a flexible linker and is buttressed by the N-terminal lobe via largely hydrophobic interactions. The strictly conserved active site, the C-H-D catalytic triad (C¹³⁷, H¹⁷², D¹⁸⁹; Fig. 3B), is located at the interface between the two halves of the protein, with the histidine and aspartate residues being contributed by the C-terminal lobe and the catalytic cysteine residue by the central helix α5 of the N-terminal lobe (Fig. 3A). The hydroxyl group of a serine residue (S¹⁹⁰) points toward the active site and engages in a hydrogen bond with D¹⁸⁹ of the catalytic triad.

The catalytic triad is equally conserved within the LapG subgroup and all BTLCPs. The residue corresponding to position 190 in *L. pneumophila* LapG can be either a serine or an asparagine residue in the LapG subset, as well as the wider BTLCP family (Fig. 3B). In order to more globally visualize the conservation of LapG-type proteases, we mapped the conservation scores of 24 LapG orthologs onto the accessible surface of the protease fold. Orthologs from distantly related species, including *Pseudomonas*,

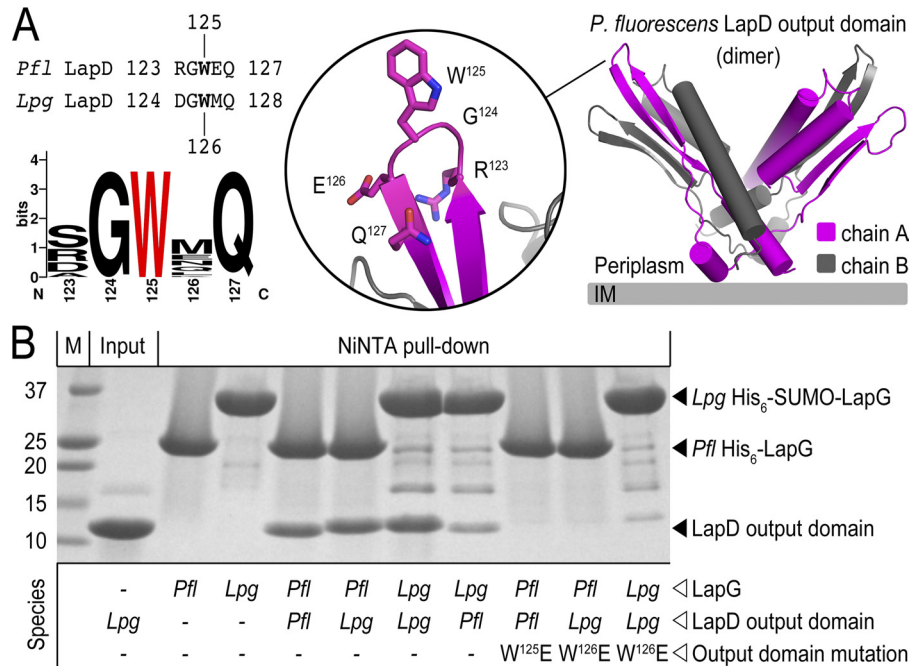


FIG 2 Conserved interaction of LapD and LapG. (A) Sequence conservation of a loop in the periplasmic output domain of LapD (PDB code 3PJV) that is critical for LapG interaction in *P. fluorescens*. (B) Interaction between LapD's output domain with LapG. Purified, His₆-tagged LapG was bound to Ni-NTA and incubated in the absence or presence of the untagged LapD output domain. Proteins from *P. fluorescens* (*Pfl*) or *L. pneumophila* (*Lpg*) were used. A specific output domain mutation (W¹²⁵E in *P. fluorescens* LapD; W¹²⁶E in *L. pneumophila* LapD) was included. Eluted complexes were analyzed by SDS-PAGE, followed by Coomassie staining.

Legionella, and *Vibrio* species, were used to create the alignment for this analysis (see Fig. S1 in the supplemental material). Interestingly, not only is the catalytic triad strictly conserved, but we also noted a fairly conserved surface patch extending from the active site (Fig. 3C). While the functional relevance remains to be established, the hydrophobic nature of this region may suggest a role as an interaction interface, for example, for substrate binding, considering its close proximity to the active site.

A structural role can be attributed to several hydrophilic residues. Consistent with the bioinformatic and modeling study of BTLCPs (13), in addition to the invariant catalytic triad, there are several conserved, polar, or charged residues that form a hydrogen bond network stabilizing some of the core secondary structure elements adjacent to the active site (N⁹¹, N⁹⁵, K¹³⁰, and N¹⁷³ in BTLCP; N¹⁰², N¹⁰⁶, K¹⁴⁴, and the aforementioned S¹⁹⁰ in *L. pneumophila* LapG) (Fig. 4). Residues with similar function but more specific to the LapG subfamily of BTLCPs are R²⁰¹ and D²⁰³ (Fig. 4B), located in the C-terminal lobe (Fig. 4A). Positioned by D²⁰³, R²⁰¹ coordinates D¹⁸⁹ of the catalytic triad. Together, these residues are part of the hydrogen bond network that coordinates D¹⁸⁹ at the active site.

A comparison against the entire PDB using the DALI server (20) was used to identify structurally related proteins. With the structure of *L. pneumophila* LapG as the search model (Fig. 5A), we identified eukaryotic protein transglutaminases as some of the closest structural neighbors (Fig. 5B; PDB codes 1g0d, 1kv3, 1ggt, and 1nud) (3, 27, 32, 40). In addition, the search identified an arylamine *N*-acetyltransferase (Fig. 5C; PDB code 2bsz) (21) and putative bacterial cysteine proteases (Fig. 5D and E; PDB codes 3isr and 3kd4) with deposited structures but no associated publi-

cation as proteins that contain a similar fold. All but one protein (the putative bacterial protease with PDB code 3kd4) display a catalytic triad that is conserved in sequence (C-H-D) and position relative to that of LapG, with the cysteine residue being located at the tip of the central helix (Fig. 5). Notably, the activity of several transglutaminases depends on the presence of calcium ions (1, 41), and calcium-binding sites have been identified in a subset of crystal structures and by modeling approaches (e.g., PDB code 1nud; Fig. 5B) (3, 6, 9). These studies identified three distinct calcium-binding sites in the human transglutaminase 3 enzyme, with site 1 being located adjacent to the active site. For transglutaminase, this site has been proposed to stabilize the enzyme, yet a similar role in LapG could not be established. However, *P. fluorescens* LapG is sensitive to EGTA treatment and requires calcium ions for the specific cleavage of its substrate, LapA (see the accompanying report [4]), suggesting a crucial function during catalysis.

Crystal structures of calcium-bound and EGTA-treated LapG. Incited by the observation that *P. fluorescens* LapG's activity depends on calcium (4) yet no bound calcium ion was apparent in the crystal structure, we initially used pattern prediction algorithms with the apo-LapG structure as the input. The MUG calcium-binding site prediction server (38) identified a patch of four conserved, negatively charged residues adjacent to the catalytic triad that had the potential to accommodate a calcium ion (Fig. 6A). While not identical in exact position, the predicted site is as close to the active site as is calcium-binding site 1, which was found to be crucial for transglutaminase function (Fig. 5B). In LapG, three of the residues, D¹³⁶, E¹³⁸, and D¹³⁹, flank C¹³⁷ of the catalytic triad, whereas the fourth residue (D¹²⁰) is less conserved and farther away with regard to the primary sequence (Fig. 6A).

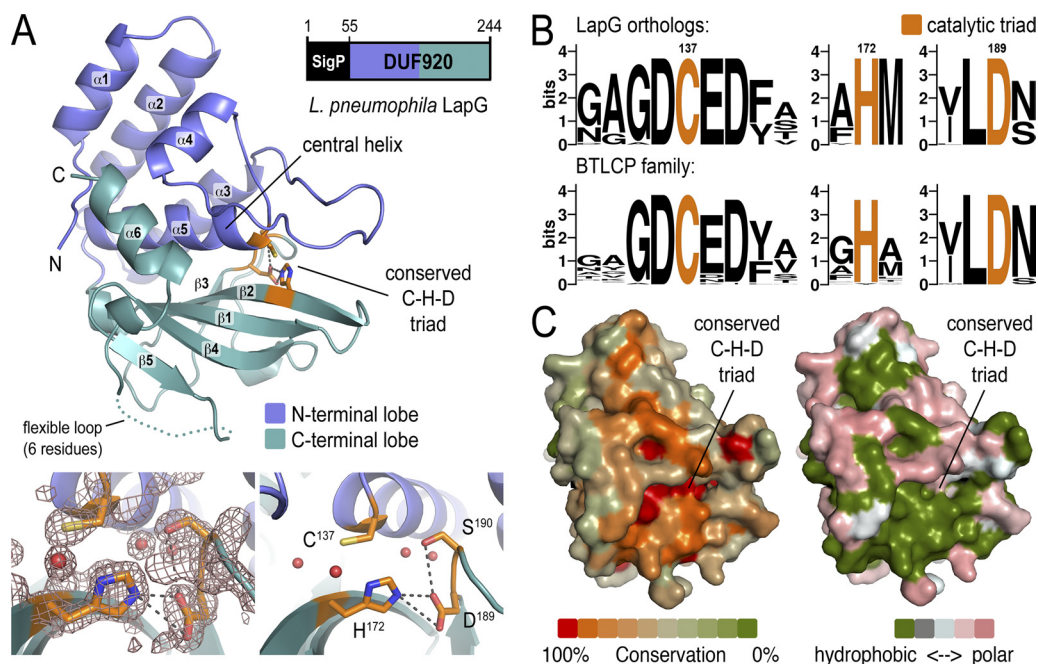


FIG 3 Crystal structure of *L. pneumophila* LapG. (A) Cartoon presentation of the LapG fold. The N- and C-terminal lobes are shown in slate and cyan, respectively. The conserved catalytic triad (cysteine-histidine-aspartate; C-H-D) is shown as sticks with the carbon atoms in orange. The electron density map at the active site (bottom left inset) has amplitudes of $2|F_o|$ to $|F_c|$, with F_o and F_c being the observed and calculated structure factors. The electron density contour is at 1.8σ . Water molecules are shown as red spheres. A hydrogen bond network involving residues of the catalytic triad is shown (bottom right inset). (B) Conservation of the catalytic triad based on the sequence alignment shown in Fig. S1 in the supplemental material. Separate sequence logos are shown for the LapG subfamily and the wider family of bacterial transglutaminase-like cysteine proteases (BTLCPs), which was generated based on an alignment that covers a representative, nonredundant set of sequences. (C) Surface conservation and hydrophobicity. Based on the alignment of 24 sequences of LapG orthologs, the sequence conservation was mapped to the accessible surface (left). In the right panel, the surface is colored according to the hydrophobicity of accessible residues. Hydrophobic residues are shown in green, and polar and charged residues are gray and pink, respectively.

However, other aspartate or glutamate residues are located in close proximity to D¹²⁰ and could function redundantly (Fig. 6A). While both the N- and C-terminal lobes contribute residues to the catalytic triad, the calcium-binding site is located entirely in the N-terminal lobe. This motif is not unique to LapG-like proteins but appears to be conserved in the entire BTLCP family on the basis of sequence alignments (Fig. 6A), indicating a general molecular mechanism of these proteases.

To confirm the prediction, we crystallized *L. pneumophila* LapG in the presence of calcium ions, yielding a new crystal form. We solved the structure by SAD phasing (space group P4₃2₁2; one molecule per asymmetric unit; see Table S2 in the supplemental material). While the maximum resolution was 1.9 Å, crystals diffracted X-rays anisotropically with a resolution of ~ 2.8 Å in the worst orientation. This observation is consistent with poor packing interactions along one crystal axis and with the two N-terminal helices being poorly resolved (with high B factors for residues 58 to 88; data not shown).

The overall fold of LapG in the new crystal form was preserved (see Fig. S2 in the supplemental material; root mean square deviation [RMSD] with or without calcium of 0.6 Å). We observed clear density around the residues predicted to form the calcium-binding site (Fig. 6B, inset). A model with a calcium ion at that site refined well. Furthermore, the coordination of the ion by the protein side chains is in good agreement with other calcium binding motifs, revealing seven ionic or polar interactions, including one water-mediated contact and a carbonyl backbone contact with

Y¹²² (Fig. 6B). To accomplish this, only the side chain of D¹²⁰ had to adopt an alternative rotamer conformation, flipping toward the binding site, while the other three residues are essentially in the same conformation as in the apo-state structure. We noticed only a small shift of the D¹²⁰-presenting loop relative to the body of LapG. However, we cannot distinguish whether this change is calcium induced or due to the altered packing interactions in this crystal form.

We also crystallized LapG treated with EGTA (see Table S2 in the supplemental material). This protein preparation crystallized in the original condition. While we obtained crystals within the same space group as LapG without EGTA treatment, it also crystallized in a second space group under identical conditions and similar crystal packing. We solved the structure by molecular replacement using the first LapG crystal structure as the search model. The structure of the EGTA-treated monomer is almost identical to the initial calcium-free state (RMSD of 0.12 Å; see Fig. S2 in the supplemental material) and very similar to the calcium-bound state despite differences in crystal contacts.

Calcium binding by *L. pneumophila* LapG. To further validate and quantify calcium binding, we turned to isothermal titration calorimetry. The titrations of calcium into a solution of LapG protein are shown in Fig. 7. Purified protein bound calcium stoichiometrically with 0.6 calcium molecule per molecule of LapG and with an affinity of 6.2 μ M (Fig. 7A; Table 1). EGTA treatment and repurification of LapG by gel filtration in EGTA-free buffer as the mobile phase yielded protein that bound calcium

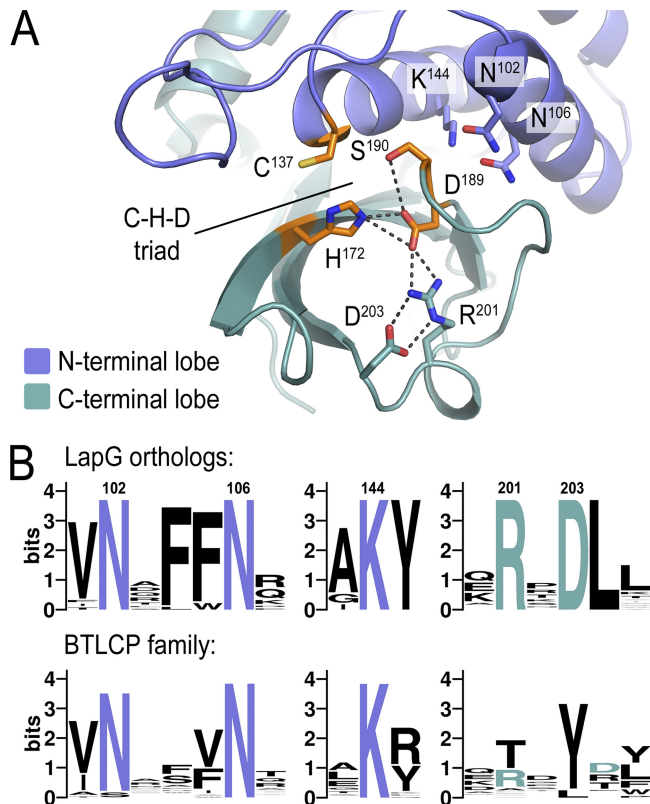


FIG 4 Conservation of a hydrogen bond network around the catalytic triad. (A) Residues from the N- and C-terminal lobes involved in a hydrogen bond network around the active site are shown as sticks. (B) Sequence conservation. Sequence logos for LapG orthologs and the entire BTLCP family are shown.

with the same affinity and negative change in enthalpy as the starting material but with a stoichiometry of close to 1 (Fig. 7A; Table 1). Together, these data indicate that LapG purifies partially bound to calcium, which can be extracted by EGTA treatment, yielding calcium-free LapG. Based on the titration data, we expect only one calcium-binding site per LapG monomer. Given that no bound calcium was observed in the initial crystal structure, we infer that the crystallization conditions are sensitive to the calcium-bound state of LapG. Finally, mutations in the key residues for calcium coordination (D¹³⁶A, E¹³⁸A, or D¹³⁹A) that were revealed by the crystal structure significantly reduce calcium binding by factors of >50 (Fig. 7B), well within the range one would expect on the basis of similar mutations in other calcium-binding proteins (39). In summary, the structural studies elucidate the overall fold, catalytic core machinery, and a calcium-binding site as conserved features of LapG-like proteases and members of the wider BTLCP superfamily.

Oligomeric state of LapG in solution. It can be assumed that the transmembrane receptor LapD, which interacts with LapG, forms a constitutive homodimer mediated at least by its HAMP domains, a two-helix module that forms a four-helix bundle within a dimeric assembly as the functional unit. This prompted us to analyze the oligomeric state of LapG in the crystals and in solution.

Two different crystal forms of calcium-free LapG were obtained, both with two molecules in their asymmetric units (RMSD of protomer A versus protomer B, 0.08 Å). A potential dimer

interface can be identified on the basis of crystal packing interactions. Although the protomer interactions are identical in the two forms (RMSD considering dimeric assemblies, 0.17 Å), the interface is marginal, spanning only 670 Å². In both crystal forms, protomers interact via a hydrophobic interface formed by the β-sheets of the C-terminal lobe (Fig. 8A). Another part of the interface in the crystallographic dimer is presented by the loop protruding from the N-terminal lobe that contains a residue involved in calcium binding (D¹²⁰), in addition to the conserved residue, D¹¹³. However, the overall packing and calculated binding enthalpies suggest that the dimerization interface is rather weak overall (23).

We next evaluated LapG's oligomerization propensity in solution by using purified proteins. We used SEC-MALS, a method that yields the absolute molecular mass of a protein as it is eluted from a gel filtration column (10). *L. pneumophila* LapG purified from *E. coli* is monomeric in solution with a molecular mass of ~25 kDa (theoretical molecular mass based on sequence, 21.6 kDa; Fig. 8B). There was no change in its monomeric state when the protein was incubated with calcium prior to SEC-MALS analysis or even when calcium was added to the mobile phase, so that calcium was present throughout the experiment.

While we observed only monomeric LapG in solution, the crystallographic dimer interface is moderately conserved across various bacterial strains (Fig. 3C; see Fig. S1 in the supplemental material), which could suggest that a subset of LapG-like orthologs may utilize this surface. Also, considering that the receptor LapD forms constitutive dimers (29), such a mode of LapG dimerization may still be relevant when LapG is bound to the output domains of intact LapD.

Conservation of the basic catalytic mechanism of LapG. Unlike in the case of *P. fluorescens*, the LapG-containing operon in *L. pneumophila* lacks a putative LapA-like substrate protein. Although the identity of the substrate for the *L. pneumophila* ortholog of LapG remains unknown, we evaluated LapG's catalytic activity by using *P. fluorescens* LapA as a model. LapA is a secreted, large adhesin protein. Previous experiments established that shorter constructs including the LapG cleavage site, a conserved TAAG motif, are processed efficiently by *P. fluorescens* LapG *in vitro* (30). The model substrate we use here comprises a 235-residue-long, N-terminal fragment of LapA with a His₆ tag at its C terminus (LapA^{Nterm}) (Fig. 9). Proteolysis of LapA^{Nterm} by purified *P. fluorescens* LapG produces a fragment of 15 kDa that can be detected by Western blotting with primary antibodies that recognize the His₆ tag. Mutation of D¹³⁴ to an alanine residue in *P. fluorescens* LapG, which corresponds to the calcium-binding mutation D¹³⁶A in *L. pneumophila* LapG, abolishes catalytic activity completely, corroborating a calcium-dependent mechanism for LapG function.

Similarly, *L. pneumophila* LapG successfully processed LapA^{Nterm}, albeit less efficiently than *P. fluorescens* LapG. In these assays, we used 100-, 250-, or 375-fold more LapG than in the samples incubated with the *P. fluorescens* protease. While we were able to detect a cleavage product with a molecular mass similar to that produced by *P. fluorescens* LapG, indicating that the same cleavage site was recognized, reaction mixtures containing *L. pneumophila* LapG still contained uncleaved substrate. In addition, we observed a second, minor cleavage product with a slightly higher molecular mass at the two highest protease concentrations, which may indicate an aspecific activity under these conditions and with this

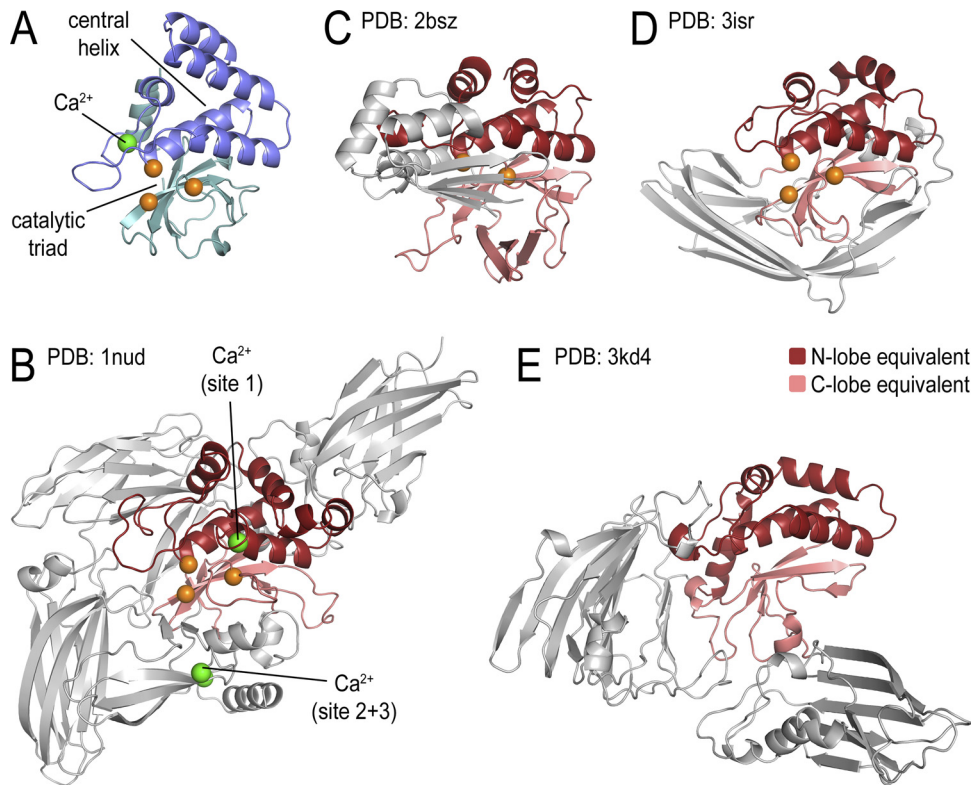


FIG 5 Structural similarities of LapG to transglutaminases, arylamine *N*-acetyltransferases, and putative bacterial proteases. A DALI protein structure database search highlighted features structurally conserved between LapG (A) and distinct classes of proteins. Regions corresponding to the N and C lobes of LapG are in red and pink, respectively, in panels B to E. Conserved catalytic (C-H-D) triads are shown as orange spheres. Calcium ions are shown as green spheres. (B) Human transglutaminase 3. Z score, 7.4; RMSD, 3.6; aligning fragment spans 135 of 673 residues. Several transglutaminases were identified. The particular structure was chosen to highlight the positions of calcium-binding sites in these enzymes. (C) *Mesorhizobium loti* arylamine *N*-acetyltransferase 1. Z score, 7.8; RMSD, 3.6; aligning fragment spans 127 of 267 residues. (D) Putative cysteine protease from *Cytophaga hutchinsonii*. Z score, 9.4; RMSD, 3.1; aligning fragment spans 121 of 285 residues. (E) Putative protease from *Parabacteroides distasonis* ATCC 8503. Z score, 7.8; RMSD, 3.2; aligning fragment spans 121 of 505 residues.

model substrate. However, proteolysis efficiency was LapG concentration dependent. Furthermore, the calcium-binding single-point mutations (D¹³⁶A, E¹³⁸A, and D¹³⁹A in *L. pneumophila* LapG) produced markedly reduced catalytic activity. Consistently, both protease orthologs failed to cleave LapA^{Nterm} when incubated with EGTA, indicating that calcium is essential for LapG's function as a periplasmic protease.

Altogether, we validated our prediction of the existing LapD-LapG system in *L. pneumophila*. More importantly, we showed that it utilizes an output and proteolytic mechanism similar to that of its *P. fluorescens* counterparts.

DISCUSSION

The superfamily of DUF920 domain-containing proteins or BTLCPs consists of more than 400 members and is conserved across the bacterial domain (13), yet functional and structural information has been scarce. We recently identified LapG as a functional example of this family, assigning it a biological role as a calcium-dependent, periplasmic protease that is involved in biofilm dispersal of *P. fluorescens* (4, 30). Since we were unable to obtain crystals of *P. fluorescens* LapG thus far, we instead determined the high-resolution crystal structure of the LapG ortholog from *L. pneumophila* in its apo and calcium-bound states. Considering the sequence conservation in functionally important motifs, the structures yield prototypic models of LapG-like proteins and the

wider family of BTLCPs. In addition, the structures confirmed their structural relationship to eukaryotic transglutaminases. In analogy to transglutaminases, LapG also shows calcium dependence, yet the exact molecular mechanism remains elusive in both cases despite the available structural data.

Calcium has been known to play myriad roles in modulating protein stability and function. In order for a protein to interact with calcium, mainly through electrostatic forces, it usually has negative charges on its surface. In the case of LapG, the N-terminal lobe displays residues D¹³⁶, E¹³⁸, and D¹³⁹, creating a highly negative surface potential with which Ca²⁺ can coordinate. It is possible that calcium binding to LapG aids in catalysis by providing increased access to the substrate or by altering enzyme structure or dynamics. While three of the four calcium-coordinating residues are strictly conserved, the fourth residue (D¹²⁰) appears more variable. On the other hand, this residue is located in a flexible loop that often harbors other, more conserved aspartate or glutamate residues in close proximity (Fig. 6), which may have a redundant calcium-coordinating function. It is possible that crystallographic packing biases the use of one position over another. The use of alternative aspartate or glutamate residues would likely impact the conformation of the loop, which could potentially alter the active or substrate-binding site. A similar mechanism has been discussed for mammalian tissue transglutaminases (26).

Another effect of calcium binding on enzyme catalysis could

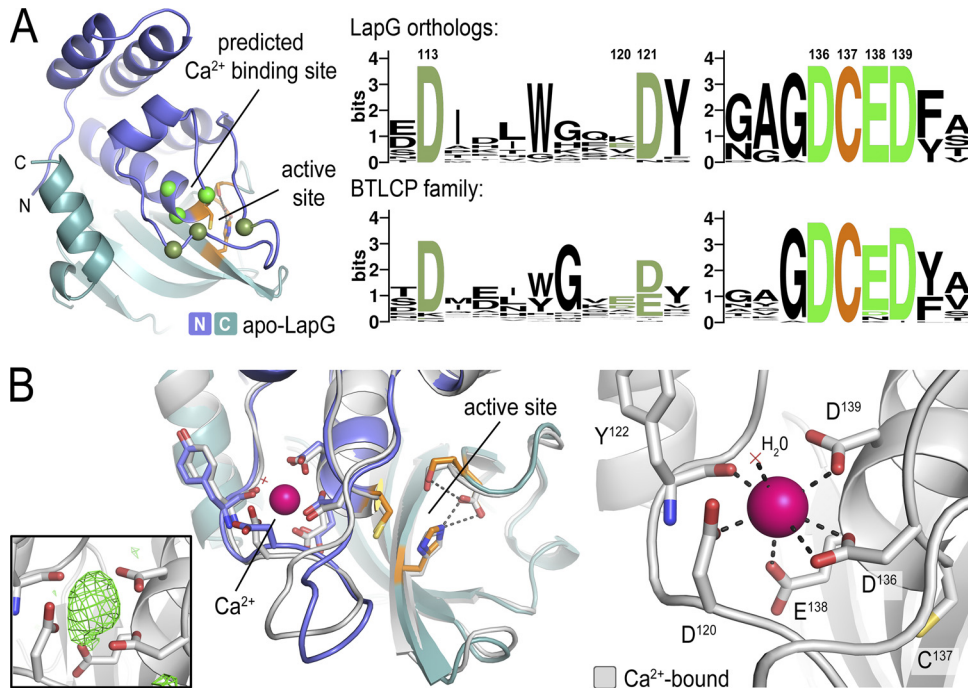


FIG 6 Structural identification of a conserved calcium-binding site in LapG. (A) Position of a putative calcium-binding site in LapG. Sequence conservation indicates that at least 3 of the 4 residues predicted to form an ion-binding site are conserved in LapG and BTLCPs. (B) Crystal structure of calcium-bound LapG. The crystal structure of LapG (gray) was determined in the presence of calcium ions (pink sphere). The left inset shows uninterpreted electron density that was observed only in the presence of calcium. The density has amplitudes of $|F_o|$ to $|F_c|$ and is contoured at 3.6σ prior to the inclusion of calcium in the refinement. The structure of non-calcium-bound LapG was superimposed. On the right, a close-up view of the calcium-binding site and calcium coordination is shown.

simply be a change in electrostatic potential close to the active site. Calcium binding is also known to influence the specific subcellular localization of proteins. For example, in the case of calpain, calcium is required for the association of the protein with cellular membranes (7). In the case here, calcium binding may preferen-

tially place LapG in close proximity to its substrate, LapA, which is anchored in the outer membrane.

The identity of the physiological target of *L. pneumophila* LapG is unknown. While the structural similarity of LapG to transglutaminases may indicate different catalytic functions, no transami-

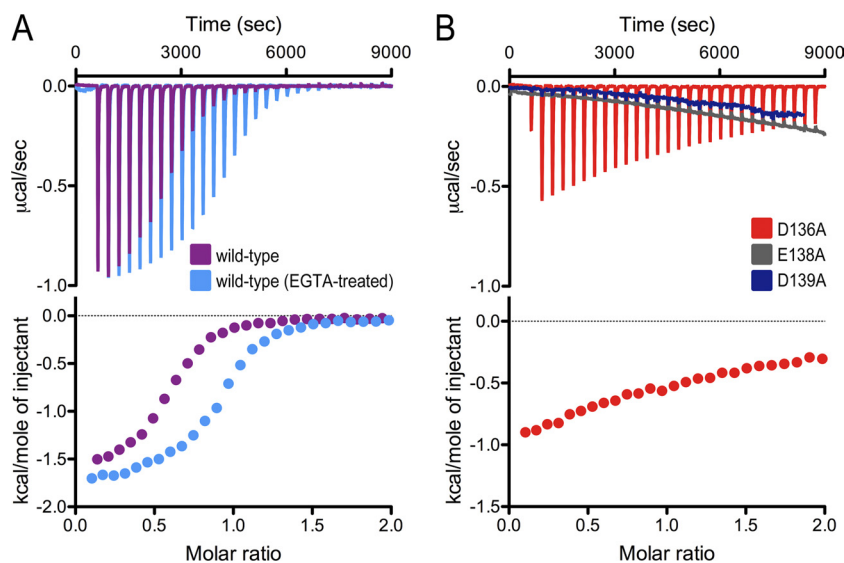


FIG 7 Isothermal titration calorimetry data for calcium binding to LapG. (A) Binding of calcium to wild-type *L. pneumophila* LapG. Calorimetric titration for calcium (2 mM) titrated into LapG (0.2 mM) is shown (top, raw data; bottom, binding isotherms). LapG purified from *E. coli* was used with or without EGTA treatment during its purification. (B) Binding of calcium to mutant LapG forms. Single-point mutations were introduced into the calcium-binding site of LapG and analyzed as described for panel A. Data analyses are summarized in Table 1.

TABLE 1 Calcium binding measured by isothermal titration calorimetry^a

<i>L. pneumophila</i> LapG	n ^b	K _d (μM)	ΔH (cal/mol)	ΔS (cal/mol/degree)
Wild type	0.59 ± 0.003	6.17 ± 0.22	-1,615 ± 10.0	18.3
EGTA-treated wild type	0.91 ± 0.005	4.98 ± 0.32	-1,720 ± 13.0	18.4
D ¹³⁶ A	0.95 ± 0.142	349.7 ± 59.3	-2,700 ± 569.9	6.6
E ¹³⁸ A	ND ^c	ND	ND	ND
D ¹³⁹ A	ND	ND	ND	ND

^a Experiments were performed at 20°C.^b n, reaction stoichiometry.^c ND, not detected.

dase activity was detected in an *in vitro* assay (D.C. and H.S., unpublished data). However, *L. pneumophila* LapG can cleave LapA^{Nterm} and thus is likely to function as a periplasmic cysteine protease. The reduced activity of *L. pneumophila* LapG for

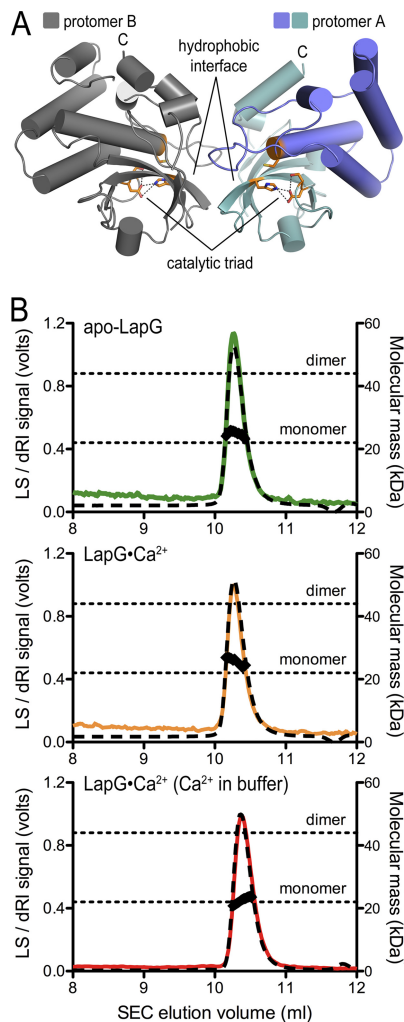


FIG 8 Oligomerization of LapG. (A) Crystallographic dimer. Analysis of crystal packing interactions reveals a putative LapG dimer that forms via partially hydrophobic interactions between protomers. (B) Oligomeric state in solution. SEC-MALS was used to determine the absolute molecular mass of LapG in solution. The effect of calcium on LapG's oligomeric state was assessed by adding calcium to the purified protein and by additionally adding calcium to the chromatography mobile phase. The averaged molecular masses were 25.1 ± 0.3 kDa for apo-LapG, 25.7 ± 0.3 kDa for LapG+Ca²⁺, and 22.5 ± 0.2 kDa for LapG with calcium in the mobile phase.

LapA^{Nterm} compared to that of the *P. fluorescens* enzyme could have several causes. Although we previously determined a consensus site for proteolytic cleavage of LapA by LapG, we also noticed that a minimal peptide containing that motif evades processing by the enzyme, suggesting that substrate recognition requires other parts of LapA (Peter D. Newell and G.A.O., unpublished data). Furthermore, *L. pneumophila* has a more complex life-style since, unlike *P. fluorescens*, it can grow autonomously or within host cells, increasing the potential target pool vastly. The notion that a putative target may be encoded outside the LapG-containing operon is supported by the presence of an incomplete type I secretion system at this *L. pneumophila* locus. Furthermore, the secretion system may be complemented by subunits encoded outside the *lapDG*-containing operon. Intracellular growth and exposure to different environments (e.g., a different pH or temperature) may also have an impact on the optimal point at which *L. pneumophila* LapG is active. Altogether, these observations hamper the identification of potential *L. pneumophila* substrates by using bioinformatics.

Yet, an interesting speculation is the possibility that LapG or related proteases could degrade host proteins or have a role not only in their own biofilm formation but also in those formed by competing

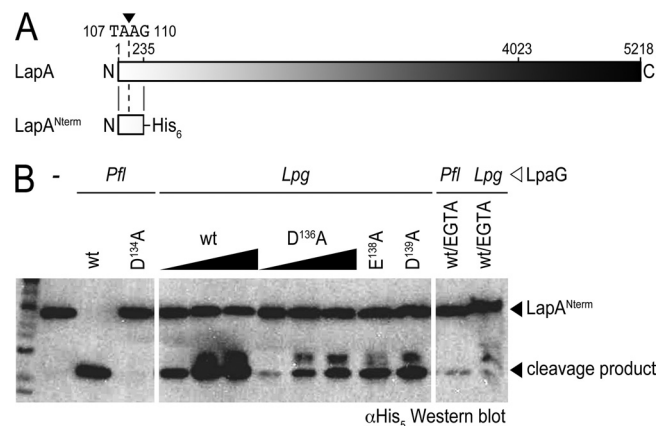


FIG 9 Proteolytic activity of *L. pneumophila* LapG. (A) A model substrate based on *P. fluorescens* LapA. Previous studies of *P. fluorescens* identified the LapG-cleavage site of LapA within the first 235 residues of the adhesin. A minimal, His₆-tagged construct containing this region (LapA^{Nterm}) was proteolyzed specifically and efficiently by *P. fluorescens* LapG. (B) *L. pneumophila* LapG activity. Site-specific cleavage of purified LapA^{Nterm} was monitored by using SDS-PAGE, followed by Western blotting with pentahistidine-specific antibodies. *L. pneumophila* LapG with the E¹³⁸A or D¹³⁹A mutation was used only at the highest concentration. *P. fluorescens* LapG and a corresponding calcium-binding mutant were included as positive and negative controls, respectively. Sensitivity to EGTA treatment was also assessed. wt, wild type.

bacteria. Substrate topology and protease access may determine the feasibility of such a model. At least in *P. fluorescens*, LapG localization to the periplasm is crucial for its regulatory effect on biofilm formation, as externally added protease does not appear to alter biofilm phenotypes (C.D.B. and G.A.O., unpublished data).

Recently, a LapADG-like system was identified in *S. oneidensis* (37). In this system, a large outer membrane protein, BpfA, is crucial for surface attachment and subsequent biofilm formation. The gene that encodes BpfA is located in a seven-gene operon which also encodes a type I secretion system, a GGDEF-EAL domain-containing protein similar to LapD, and a hypothetical conserved BTLCP-like protein homologous to LapG. An interesting finding pertains to a positive effect of calcium on *S. oneidensis* biofilm formation, which is BpfA dependent. Considering the presence of putative calcium-binding sites in LapA and BpfA, these large adhesion proteins could function as sinks for calcium ions that, in turn, are required for proteolytic processing via LapG-like proteases. Such a mechanism is supported by the observation that bacteria have the ability to concentrate calcium in their periplasm to levels that are comparable to or above the measured affinity of LapG for calcium (22). Although the exact mechanism by which these proteins interact and function has yet to be established, it is quite possible that they are regulated in a fashion very similar to that of the Lap system in *P. fluorescens* (4, 29, 30).

Although the corresponding regulators and mechanism remain elusive for the orthologous system in *L. pneumophila*, a growth phenotype in macrophages has been observed upon the overexpression of CdgS9, the LapD ortholog in *L. pneumophila*, indicating that the system is operational in this opportunistic pathogen (25). In particular, cells showed a moderate or severe growth reduction in rich broth or in macrophages, respectively. Our structural and mechanistic studies described here may facilitate future research to uncover the physiological role of this system in *L. pneumophila* and other bacteria. The protease and its interaction with the receptor LapD/CdgS9 also provide an attractive angle for the development of specific inhibitors.

ACKNOWLEDGMENTS

We are grateful to Howard Shuman for providing genomic DNA and to William Horne for providing access to isothermal titration calorimetry.

This work is based upon research conducted at the CHES. The facility is supported by grant DMR-0225180 from the National Science Foundation (NSF) and grant RR-01646 from the National Institutes of Health (NIH). Our work was supported by the NIH under grants R01-GM081373 (H.S.), R01-AI097307 (G.A.O. and H.S.), and T32 GM08704 (C.D.B.); by the NSF under grant MCB-9984521 (G.A.O.); and by a PEW scholar award in Biomedical Sciences (H.S.).

REFERENCES

- Achyuthan KE, Greenberg CS. 1987. Identification of a guanosine triphosphate-binding site on guinea pig liver transglutaminase. Role of GTP and calcium ions in modulating activity. *J. Biol. Chem.* 262:1901–1906.
- Adams PD, et al. 2010. PHENIX: a comprehensive Python-based system for macromolecular structure solution. *Acta Crystallogr. D Biol. Crystallogr.* 66:213–221.
- Ahvazi B, Boeshans KM, Idler W, Baxa U, Steinert PM. 2003. Roles of calcium ions in the activation and activity of the transglutaminase 3 enzyme. *J. Biol. Chem.* 278:23834–23841.
- Boyd CD, Chatterjee D, Sondermann H, O'Toole GA. 2012. LapG, required for modulating biofilm formation by *Pseudomonas fluorescens* Pf0-1, is a calcium-dependent protease. *J. Bacteriol.* 194:4406–4414.
- Carlson HK, Vance RE, Marletta MA. 2010. H-NOX regulation of c-di-GMP metabolism and biofilm formation in *Legionella pneumophila*. *Mol. Microbiol.* 77:930–942.
- Casadio R, et al. 1999. The structural basis for the regulation of tissue transglutaminase by calcium ions. *Eur. J. Biochem.* 262:672–679.
- Croall DE, Ersfeld K. 2007. The calpains: modular designs and functional diversity. *Genome Biol.* 8:218. doi:10.1186/gb-2007-8-6-218.
- Crooks GE, Hon G, Chandonia JM, Brenner SE. 2004. WebLogo: a sequence logo generator. *Genome Res.* 14:1188–1190.
- Datta S, Antonyak MA, Cerione RA. 2006. Importance of Ca(2+)-dependent transamidation activity in the protection afforded by tissue transglutaminase against doxorubicin-induced apoptosis. *Biochemistry* 45:13163–13174.
- De N, Navarro MV, Wang Q, Krasteva PV, Sondermann H. 2010. Biophysical assays for protein interactions in the Wsp sensory system and biofilm formation. *Methods Enzymol.* 471:161–184.
- Emsley P, Cowtan K. 2004. Coot: model-building tools for molecular graphics. *Acta Crystallogr. D Biol. Crystallogr.* 60:2126–2132.
- Galperin MY, Nikolskaya AN, Koonin EV. 2001. Novel domains of the prokaryotic two-component signal transduction systems. *FEMS Microbiol. Lett.* 203:11–21.
- Ginalski K, Kinch L, Rychlewski L, Grishin NV. 2004. BTLCP proteins: a novel family of bacterial transglutaminase-like cysteine proteinases. *Trends Biochem. Sci.* 29:392–395.
- Gjermansen M, Nilsson M, Yang L, Tolker-Nielsen T. 2010. Characterization of starvation-induced dispersion in *Pseudomonas putida* biofilms: genetic elements and molecular mechanisms. *Mol. Microbiol.* 75:815–826.
- Gouet P, Courcelle E, Stuart DI, Metz F. 1999. ESPript: analysis of multiple sequence alignments in PostScript. *Bioinformatics* 15:305–308.
- Hall-Stoodley L, Costerton JW, Stoodley P. 2004. Bacterial biofilms: from the natural environment to infectious diseases. *Nat. Rev. Microbiol.* 2:95–108.
- Hengge R. 2009. Principles of c-di-GMP signalling in bacteria. *Nat. Rev. Microbiol.* 7:263–273.
- Hinsa SM, Espinosa-Urgel M, Ramos JL, O'Toole GA. 2003. Transition from reversible to irreversible attachment during biofilm formation by *Pseudomonas fluorescens* WCS365 requires an ABC transporter and a large secreted protein. *Mol. Microbiol.* 49:905–918.
- Hinsa SM, O'Toole GA. 2006. Biofilm formation by *Pseudomonas fluorescens* WCS365: a role for LapD. *Microbiology* 152:1375–1383.
- Holm L, Rosenstrom P. 2010. Dali server: conservation mapping in 3D. *Nucleic Acids Res.* 38:W545–W549.
- Holton SJ, et al. 2005. Structure of *Mesorhizobium loti* arylamine N-acetyltransferase 1. *Acta Crystallogr. Sect. F Struct. Biol. Cryst. Commun.* 61(Pt 1):14–16.
- Jones HE, Holland IB, Campbell AK. 2002. Direct measurement of free Ca(2+) shows different regulation of Ca(2+) between the periplasm and the cytosol of *Escherichia coli*. *Cell Calcium* 32:183–192.
- Krissinel E, Henrick K. 2007. Inference of macromolecular assemblies from crystalline state. *J. Mol. Biol.* 372:774–797.
- Larkin MA, et al. 2007. Clustal W and Clustal X version 2.0. *Bioinformatics* 23:2947–2948.
- Levi A, Folcher M, Jenal U, Shuman HA. 2011. Cyclic diguanylate signaling proteins control intracellular growth of *Legionella pneumophila*. *mBio* 2:e00316–00310. doi:10.1128/mBio.00316-10.
- Li B, Cerione RA, Antonyak M. 2011. Tissue transglutaminase and its role in human cancer progression. *Adv. Enzymol. Relat. Areas Mol. Biol.* 78:247–293.
- Liu S, Cerione RA, Clardy J. 2002. Structural basis for the guanine nucleotide-binding activity of tissue transglutaminase and its regulation of transamidation activity. *Proc. Natl. Acad. Sci. U. S. A.* 99:2743–2747.
- Monds RD, Newell PD, Gross RH, O'Toole GA. 2007. Phosphate-dependent modulation of c-di-GMP levels regulates *Pseudomonas fluorescens* Pf0-1 biofilm formation by controlling secretion of the adhesin LapA. *Mol. Microbiol.* 63:656–679.
- Navarro MV, et al. 2011. Structural basis for c-di-GMP-mediated inside-out signaling controlling periplasmic proteolysis. *PLoS Biol.* 9:e1000588. doi:10.1371/journal.pbio.1000588.
- Newell PD, Boyd CD, Sondermann H, O'Toole GA. 2011. A c-di-GMP effector system controls cell adhesion by inside-out signaling and surface protein cleavage. *PLoS Biol.* 9:e1000587. doi:10.1371/journal.pbio.1000587.
- Newell PD, Monds RD, O'Toole GA. 2009. LapD is a bis-(3',5')-cyclic

- dimeric GMP-binding protein that regulates surface attachment by *Pseudomonas fluorescens* Pf0-1. Proc. Natl. Acad. Sci. U. S. A. **106**: 3461–3466.
32. Noguchi K, et al. 2001. Crystal structure of red sea bream transglutaminase. J. Biol. Chem. **276**:12055–12059.
 33. Otwinowski Z, Minor W. 1997. Processing of X-ray diffraction data collected in oscillation mode. Macromol. Crystallogr. A **276**:307–326.
 34. Plate L, Marletta MA. 2012. Nitric oxide modulates bacterial biofilm formation through a multicomponent cyclic-di-GMP signaling network. Mol. Cell **46**:449–460.
 35. Schneider TD, Stephens RM. 1990. Sequence logos: a new way to display consensus sequences. Nucleic Acids Res. **18**:6097–6100.
 36. Sondermann H, Shikuma NJ, Yildiz FH. 2012. You've come a long way: c-di-GMP signaling. Curr. Opin. Microbiol. **15**:140–146.
 37. Theunissen S, et al. 2010. The 285 kDa Bap/RTX hybrid cell surface protein (SO4317) of *Shewanella oneidensis* MR-1 is a key mediator of biofilm formation. Res. Microbiol. **161**:144–152.
 38. Wang X, Kirberger M, Qiu F, Chen G, Yang JJ. 2009. Towards predicting Ca²⁺-binding sites with different coordination numbers in proteins with atomic resolution. Proteins **75**:787–798.
 39. Yang JJ, Gawthrop A, Ye Y. 2003. Obtaining site-specific calcium-binding affinities of calmodulin. Protein Pept. Lett. **10**:331–345.
 40. Yee VC, et al. 1994. Three-dimensional structure of a transglutaminase: human blood coagulation factor XIII. Proc. Natl. Acad. Sci. U. S. A. **91**: 7296–7300.
 41. Zhang J, Lesort M, Guttman RP, Johnson GV. 1998. Modulation of the in situ activity of tissue transglutaminase by calcium and GTP. J. Biol. Chem. **273**:2288–2295.